

Nuclear effects on the extraction of neutron structure functions

I. Schmidt^{1,a} J.-J. Yang^{1,2,b}

¹ Departamento de Física, Universidad Técnica Federico Santa María, Casilla 110-V, Valparaíso, Chile

² Department of Physics, Nanjing Normal University, Nanjing 210097, P.R. China

Received: 1 December 2000 / Revised version: 15 February 2001 /
Published online: 25 April 2001 – © Springer-Verlag / Società Italiana di Fisica 2001

Abstract. Nuclear effects due to the presence of spin-1 isosinglet 6-quark clusters in the deuteron on the extraction of both spin-independent and spin-dependent neutron structure functions are investigated. The x -dependences of the 6-quark cluster structure functions are estimated by using a perturbative QCD (pQCD) dimensional counting rules. Within this framework, the ratio of the deuteron structure function to the free nucleon structure function can be well described. We find that the nuclear effect on the extracted spin-dependent neutron structure function is very different from that on the spin-independent neutron structure function. The effect enhances the Bjorken sum by about 10%, whereas it decreases the Gottfried sum by about 7%. The formalism for calculating nuclear effects is further used to evaluate the spin-dependent structure function of the ^3He nucleus and a good self-consistent check is obtained.

1 Introduction

It has been commonly accepted that the nuclear corrections are important in extracting the neutron structure functions from deuteron and ^3He data [1]. Some years ago, the New Muon Collaboration (NMC) [2,3] reported a value of the Gottfried sum, using the ratio $F_2^n/F_2^p = 2F_2^D/F_2^p - 1$, where nuclear effects in the deuteron target were neglected, and its structure function was regarded as the sum of the structure functions of the proton and neutron. Then the neutron structure function F_2^n can be extracted, and the ratio of the deuteron structure function F_2^D to the free nucleon structure function $F_2^N = (F_2^p + F_2^n)/2$ should read $R_F^{D/N} = 1$. However, Gomez et al. [4] found that the deuteron has a significant EMC effect [5], i.e. $R_F^{D/N} \neq 1$, especially in the region near $x \sim 0.6$. In addition, the result of E665 measurement [6] suggests the presence of nuclear shadowing effects in the deuteron. The analysis of Epele et al. [7] also shows a significant nuclear effect due to the composite nature of the deuteron. In fact, the importance of nuclear effects on the extraction of the neutron structure functions was recognized even much earlier [8]. Recent investigations of nuclear effects on a deuteron mainly emphasize the following three aspects:

- (1) the EMC effect on the spin-independent deuteron structure function [4,9,10];
- (2) the effects of Fermi motion of the nucleons in the deuteron [11–13];
- (3) depolarization of the nucleons and spin-dependent effects [14].

In recent work by Burov and Molochkov [9], the EMC effect on a deuteron was analyzed from a relativistic point of view. Fermi motion for the spin-independent F_2^D and F_3^D structure functions in light-cone variables was analyzed in [11] and [12], respectively. The same relativistic approach and a deuteron model have been used [13] in order to describe the effect of Fermi motion corrections to the spin-dependent structure function g_1^D , and to estimate nuclear effects in the $\mu + D \rightarrow \mu + X$ process. But there have been no detailed studies of the possible nuclear effects on the extraction of the neutron structure functions (F_2^n, g_1^n). Nuclear effects including Fermi motion and shadowing are crucially important in order to extract the neutron deep-inelastic structure functions from the experimental data for deuteron and heavy nuclei. They should be included into any QCD analysis of the nucleon structure functions. The main purpose of our present work is to investigate nuclear effects on the extraction of the neutron structure functions.

Generally, it is hard to give a unified description of all nuclear effects including Fermi motion corrections at large x , and shadowing and anti-shadowing effects in the small x region. The work by Lassila and Sukhatme [15] shows that the quark cluster model (QCM) can be used to model the EMC effect over all x . The QCM has been successfully applied to inclusive electron deuteron reactions at large momentum transfer, and to nuclear Drell–Yan processes. Spin-dependent effects in the quark cluster model of the deuteron and ^3He were investigated by Benesh and Vary [14]. However, in [14] there were no detailed 6-quark clusters quark distributions, and hence only the first moment

Correspondence to: I. Schmidt

^a e-mail: ischmidt@fis.utfsm.cl

^b e-mail: jjyang@fis.utfsm.cl

of a particular distribution was involved in the estimation. In order to get more precise information of nuclear effects on the extraction of the neutron structure functions, detailed quark distributions of 6-quark clusters are necessary. This motivates us to construct the quark distributions of 6-quark clusters. Several years ago, Brodsky, Burkardt and Schmidt provided a reasonable description of the spin-dependent quark distributions of the nucleon in a pQCD based model [16]. This model has also been successfully used in order to explain the large single-spin asymmetries found in semi-inclusive pion production in pp collisions, while other models have not been able to fit the data [17]. Recently it has also been applied to obtain a good description of the spin and flavor structure of octet baryons [18], specially the Λ particle [19–21]. In this paper, we extend this analysis to 6-quark clusters, trying to describe its spin-dependent quark distributions within this framework.

The spin-dependent structure functions are interesting not only because they introduce a new physical variable with which one can explore the detailed structure of the nucleon, but also because they provide a precise test of QCD via the Bjorken sum rule, which is a strict QCD prediction. In this paper, we address nuclear effects on the extraction of the neutron spin-dependent structure function in the quark cluster model of the deuteron and ${}^3\text{He}$. We will show that nuclear effects cause a big enhancement of the Bjorken sum by about 10%, giving a final result which is much closer to the theoretical value of the Bjorken sum rule.

This paper is organized as follows. In Sect. 2 we will describe the quark distributions of a 6-quark cluster in the pQCD based model. In Sect. 3 we estimate the nuclear effects due to the presence of 6-quark clusters in the deuteron, and on the corresponding extraction of the spin-independent neutron structure function F_2^n . The ratio of the deuteron structure function to the free nucleon structure function and the effect on the Gottfried sum are calculated. We find that our model can give a very good unified description of the nuclear effects in the deuteron structure function and that the nuclear effect decreases the Gottfried sum by about 7%. In Sect. 4 we present an analysis of the possible effect on the extraction of the spin-dependent neutron structure function and the Bjorken sum. A significant effect on the spin-dependent neutron structure function, and therefore on the Bjorken sum, is obtained. The formalism for calculation the nuclear effect is checked by applying it to the ${}^3\text{He}$ nucleus. Finally, a discussion and summary are included in Sect. 5.

2 Quark distributions in spin-1 isosinglet 6-quark cluster

We use a simple model in which there is a small probability of finding the deuteron in a 6-quark cluster state, which allows for the overlap of nucleons.

In order to describe the spin-dependent quark distributions of the nucleon, Brodsky, Burkardt and Schmidt

developed a pQCD based model [16]. Here we extend this analysis to the description of the quark distributions in a 6-quark cluster. In the region $z \rightarrow 1$, where z is the light-cone momentum fraction carried by a given quark or antiquark in the 6-quark cluster ($0 \leq z \leq 1$), pQCD can give rigorous predictions for the behavior of distribution functions. In particular, it predicts “helicity retention”, which means that the helicity of a valence quark will match that of the parent quark cluster. Explicitly the quark distributions of a spin-1 isosinglet 6-quark cluster satisfy the counting rule [22]

$$Q_6(z) \sim (1-z)^p, \quad (1)$$

where

$$p = 2n - 1 + 2\Delta S_z. \quad (2)$$

Here n is the minimal number of the spectator quarks, and $\Delta S_z = |S_z^q - S_z^{\bar{q}}| = 1/2$ or $3/2$ for parallel or anti-parallel quark and the 6-quark cluster helicities, respectively. More specifically, following [16], spin distributions for the non-strange quarks in the 6-quark cluster are parameterized as

$$Q_6^\uparrow(z) = \frac{1}{z^\alpha} [A_6(1-z)^{10} + B_6(1-z)^{11}], \quad (3)$$

$$Q_6^\downarrow(z) = \frac{1}{z^\alpha} [C_6(1-z)^{12} + D_6(1-z)^{13}]. \quad (4)$$

Here the distributions include both the quark and antiquark contributions, i.e. $Q = q + \bar{q}$, and q is regarded as the sum of the non-strange quarks, i.e. $q = u + d$, since there are no detailed experimental data guiding us to determine separate quark distributions in the 6-quark cluster. The effective QCD Pomeron intercept $\alpha = 0.8$ is introduced to reflect the Regge behavior at low z . There are four parameters for the above quark distributions. Since the nucleon overlap region is small, we make the assumption that in the formation of the 6-quark cluster the quarks retain approximately the total helicity and momentum they had in the nucleons. Therefore we fix the parameters by using the following conditions: one condition arises from the requirement that the sum rules converge at $z \rightarrow 0$; the second condition from the values of the integral of the polarized quark distribution $\Delta Q_6 = 0.68$ which is $2(\Delta u + \Delta d)$ of the nucleon [23]; the third condition reflects the fact that the momentum fraction z_Q carried by the quark and antiquark of a 6-quark cluster should be half of that for a single nucleon, i.e., $z_Q = \frac{1}{2}(x_u + x_d) = 0.2605$ [24]. This leaves us with one unknown, which is chosen to be C_6 . The three constraints give the solution set

$$\begin{aligned} A_6 &= 0.9937C_6 + 8.9047, \\ B_6 &= -1.0948C_6 - 6.3505, \\ D_6 &= -1.1011C_6 + 2.5542. \end{aligned} \quad (5)$$

The probabilistic interpretation of the parton distributions Q_6^\uparrow and Q_6^\downarrow implies the bounds

$$0 < C_6 < 25.26. \quad (6)$$

Similarly, the strange quark and anti-quark distributions are parameterized as

$$S_6^\uparrow(z) = \frac{1}{z^{\alpha'}} [A_s(1-z)^{12} + B_s(1-z)^{13}], \quad (7)$$

$$S_6^\downarrow(z) = \frac{1}{z^{\alpha'}} [C_s(1-z)^{14} + D_s(1-z)^{15}], \quad (8)$$

with

$$\begin{aligned} A_s &= 0.9959C_s - 3.6213, \\ B_s &= -1.0678C_s + 3.9005, \\ D_s &= -1.0720C_s + 0.2792, \end{aligned} \quad (9)$$

which are constrained by

- (1) the requirement that the sum rules converge at $z \rightarrow 0$;
- (2) the values of $\Delta S_6 = -0.24$, twice as large as the value $\Delta S = -0.12$ for the nucleon [23];
- (3) the sum of momentum fractions carried by the strange quarks and anti-quarks, $z_s = 0.0175$, half of the value $x_s = 0.035$ for the nucleon [16].

$\alpha' = 1$ Regge behavior for sea quarks is adopted. The probabilistic interpretation of the parton distributions S_6^\uparrow and S_6^\downarrow requires

$$3.637 < C_s < 3.879. \quad (10)$$

In the following calculation, first we consider only the contributions of non-strange quarks and we find that the value $C_6 = 10$ can be taken to fit the data of the ratio of the deuteron structure function to the free nucleon structure function. Then we investigate the effect due to the presence of the strange quark.

3 Nuclear effects on extraction of spin-independent neutron structure function

Nuclear effects on the extracted neutron structure function will be indicated by the ratio $R_F^{D/N}$ of the deuteron structure function to the free nucleon structure function, and the modification of the Gottfried sum.

3.1 Ratio $R_F^{D/N}$

The EMC effect indicates that there is overlap of nucleons and the existence of 6-quark clusters in a nucleus. Now we will use the above 6-quark cluster quark distributions in order to understand the nuclear effects in the deuteron structure function.

The probability for creating a 6-quark cluster in the deuteron has been calculated as $p_6 = 0.054$ [14]. We use a simple model where a fraction p_6 of the nucleons in deuterium have become part of a 6-quark cluster, with a fraction $(1-p_6)$ remaining single nucleons. In order to compare with the experimental data, we introduce the ratio

$$R_F^{D/N} = \frac{F_2^D}{\tilde{F}_2^N}, \quad (11)$$

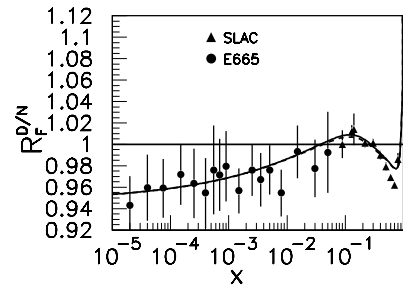


Fig. 1. The ratio $R_F^{D/N}(x)$ and the comparison with the E665 data [6] and the SLAC data from [4]. Dashed and solid curves correspond to including only contributions of non-strange quarks, and including also the contribution of the strange quark in the 6-quark cluster, respectively

where

$$\tilde{F}_2^N = \frac{1}{2}(F_2^p + \tilde{F}_2^n), \quad (12)$$

with

$$\tilde{F}_2^n(x) = \frac{[2F_2^D(x) - p_6\tilde{F}_2^6(\frac{x}{2})]}{1-p_6} - F_2^p(x), \quad (13)$$

assuming that the clusters formed in the s -wave and d -wave components have the same structure [14]. We denote the neutron structure function as \tilde{F}_2^n , which is different from F_2^n , extracted via

$$F_2^n(x) = 2F_2^D(x) - F_2^p(x), \quad (14)$$

without considering nuclear effects. In (13), the structure function of the 6-quark cluster can be expressed as

$$\tilde{F}_2^6(z) = \frac{z}{9}[5Q_6(z) + 2S_6(z)], \quad (15)$$

where

$$Q_6(z) = Q_6^\uparrow(z) + Q_6^\downarrow(z), \quad (16)$$

and

$$S_6(z) = S_6^\uparrow(z) + S_6^\downarrow(z). \quad (17)$$

In (13) and (14), the deuteron structure function F_2^D and the proton structure function F_2^p are taken from the parametrizations of NMC [25]. Our numerical calculations show that the effect of the strange quark is very small. In order to understand the data of $R_F^{D/N}$ at $Q^2 = 4 \text{ GeV}^2$, the one free parameter for the non-strange quark distribution Q_6 of the 6-quark cluster should be chosen as $C_6 = 10$. In Fig.1 we present the calculated results of the ratio $R_F^{D/N}$, together with the E665 data [6] and the SLAC data which were extracted by Gomez et al. [4] using a model of Frankfurt and Strikman [26]. We obtain a good unified description of the nuclear effects including shadowing, anti-shadowing at small x and Fermi motion at large x , with the presence of 6-quark clusters.

The nuclear shadowing effect has been described well by multiple scattering of hadronic fluctuation of the virtual photon with nucleons inside a target nucleus in the

target rest frame or by parton recombinations in the infinite momentum frame [1,27–29]. Although we describe the nuclear shadowing by introducing an admixture of 6-quark clusters in the nucleus, our model is related to other successful approaches such as the parton recombination picture. In the infinite momentum frame, the longitudinal localization size of a parton with the momentum xp_N can be expressed as $L = 1/(xp_N)$. If a parton has a small x and consequently its dimension (L) exceeds the nucleon longitudinal size, it leaks out of the nucleon and recombines with partons of other nucleons. This is the nuclear shadowing mechanism of the parton recombination picture. In our description, partons from different neighboring nucleons meet in the spatial overlap between the nucleons in the nucleus and re-distribute there with pQCD counting rules. For partons with small x , they recombine by fusion due to their high density in the overlapping region. In our view, during the formation of a 6-quark cluster, the recombination of small x partons in the spatial overlap of neighboring nucleons results in nuclear shadowing effect. Our model can give a good description of the nuclear shadowing effect as well as the parton recombination picture since its dynamic mechanism is closely related to the parton recombination.

Now, let us turn to the understanding of the nuclear effect in medium and large x regions. The quarks in a 6-quark cluster have a larger confinement size than those in the nucleon, which leads to the redistribution of the quarks towards to the lower momentum end, i.e. a lower x region according to the uncertainty principle. This causes a suppression of the quark distributions in the medium x region and an enhancement in the low x region. The competition of the enhancement effect with the shadowing effect leads to the anti-shadowing effect at $x \sim 0.1$. A rise of the ratio at large x is expected from Fermi motion of the nucleons, and this is related to the nuclear wave function for overlapping nucleons which is here modeled as a 6-quark cluster. The nuclear effects over all x have been unified and modeled as the presence of the 6-quark clusters in the deuteron. The strange quark in the 6-quark clusters only gives a very small modification, and there is no significant change in its effect when the free parameter C_s varies in the admissible range [3.637, 3.879]. For simplicity, we only show the strange contribution with $C_s = 3.8$ in the following results.

3.2 The effect on the Gottfried sum

Recently, the New Muon Collaboration (NMC) experiment [2] has provided values for the ratio of the structure function F_2^n/F_2^p , assuming that nuclear effects are not significant in the deuteron, i.e.,

$$F_2^p - F_2^n = 2F_2^D \frac{1 - F_2^n/F_2^p}{1 + F_2^n/F_2^p}, \quad (18)$$

where

$$\frac{F_2^n}{F_2^p} = 2 \frac{F_2^D}{F_2^p} - 1. \quad (19)$$

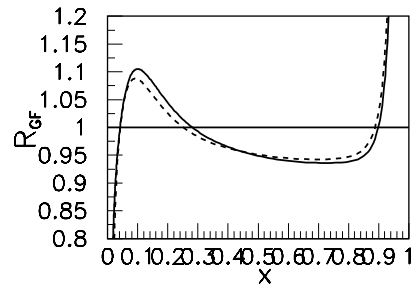


Fig. 2. The ratio $R_{GF}(x)$. Dashed and solid curves correspond to including only contributions of non-strange quarks, and including also the contribution of the strange quark in 6-quark clusters, respectively

The Gottfried sum is defined as [30]

$$S_{GS} = \int S_{GF}(x) dx, \quad (20)$$

with the Gottfried integrand function given by

$$S_{GF}(x) = \frac{(F_2^p(x) - F_2^n(x))}{x}. \quad (21)$$

When we allow for the presence of 6-quark clusters in the deuteron, the neutron structure function should be extracted as \tilde{F}_2^n from (13). The corresponding Gottfried integrand should be modified from S_{GF} to

$$\tilde{S}_{GF}(x) = \frac{(F_2^p(x) - \tilde{F}_2^n(x))}{x}. \quad (22)$$

In order to visualize the nuclear effects, the ratio

$$R_{GF}(x) = \frac{\tilde{S}_{GF}(x)}{S_{GF}(x)} \quad (23)$$

is shown in Fig. 2. Taking the minimal value of x as $x_{\min} = 0.004$, which corresponds to the kinematic limit of the experiment in [3], we obtain the value of the Gottfried sum,

$$S_{GS} = \int_{0.004}^1 S_{GF}(x) dx = 0.223, \quad (24)$$

and

$$\tilde{S}_{GS} = \int_{0.004}^1 \tilde{S}_{GF}(x) dx = 0.204, \quad (25)$$

without taking into account the contribution of the strange quarks in the 6-quark clusters. We find an approximate 8.5% suppression in the Gottfried sum due to nuclear effects. When the contribution of the strange quark is also included with $C_s = 3.8$, we find that the Gottfried sum becomes $\tilde{S}_{GS} = 0.208$, i.e. the nuclear effect decreases the Gottfried sum by about 7%. It has been commonly accepted that the nuclear modification to the Gottfried sum predominantly comes from the small x nuclear shadowing

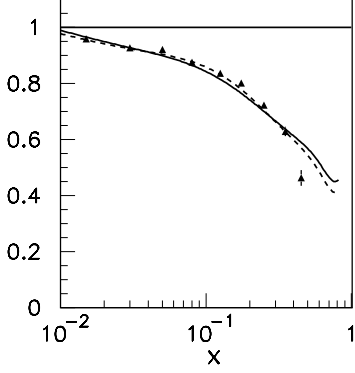


Fig. 3. The ratios F_2^n/F_2^p and \tilde{F}_2^n/F_2^p are shown in dashed and solid curves, respectively. The neutron structure function is extracted from the deuteron structure function F_2^D and the proton structure F_2^p which are taken from the parametrizations of NMC [25]. Experimental data are taken from [3]

region. Hence our above estimate is consistent with a 4–10% decrease in the value of the Gottfried sum due to the shadowing correction [31].

In addition, the ratio of the structure function of the neutron to that of the proton is shown in Fig. 3. The $x \rightarrow 1$ behavior of the neutron to proton structure function ratio is an important result which can differentiate between different nucleon structure models [32]. For example, in exact SU(6) its value is $2/3$, in some diquark models it is $1/4$ [33], while pQCD predicts $3/7$ [34, 16]. Our analysis favors the pQCD prediction.

4 Nuclear effects on extraction of spin-dependent neutron structure function

Similar to the spin-independent case, we will consider the same nuclear effects on the extraction of the neutron spin-dependent structure function. We will indicate these effects by presenting the result of the ratio $R_g^{D/N}$ of deuteron spin-dependent structure function to the free nucleon spin-dependent structure function, and the correction to the Bjorken sum.

4.1 Ratio $R_g^{D/N}$

In the absence of 6-quark clusters, only the depolarization of the proton and neutron in the d -wave component of the deuteron wave function will be taken into account, and hence the spin-dependent structure function can be written as

$$g_1^D(x) = \left(p_s - \frac{1}{2}p_d \right) \frac{[g_1^p(x) + g_1^n(x)]}{2}, \quad (26)$$

where p_s and p_d denote the probabilities for finding the deuteron in an s - or d -wave, respectively. If we allow for

the existence of 6-quark clusters in deuterium, $g_1^D(x)$ becomes [14]

$$g_1^D(x) = \left[(p_s - p_{6s}) - \frac{1}{2}(p_d - p_{6d}) \right] \frac{[g_1^p(x) + \tilde{g}_1^n(x)]}{2} + \frac{1}{2}p_6g_1^6\left(\frac{x}{2}\right), \quad (27)$$

where $p_{6s} = 0.047$ and $p_{6d} = 0.007$, the probabilities for creating a 6-quark cluster in the s - and d -states, were calculated by Benesh and Vary [14], $p_6 = p_{6s} + p_{6d}$, and g_1^6 is the spin-dependent structure function of a spin-1, isosinglet 6-quark cluster,

$$g_1^6(z) = \frac{1}{18}[5\Delta Q_6(z) + 2\Delta S_6(z)], \quad (28)$$

where

$$\Delta Q_6(z) = Q_6^\uparrow(z) - Q_6^\downarrow(z), \quad (29)$$

and

$$\Delta S_6(z) = S_6^\uparrow(z) - S_6^\downarrow(z). \quad (30)$$

From (26) and (27), both g_1^n and \tilde{g}_1^n can be extracted, without 6-quark clusters and with 6-quark clusters, respectively. The first moment of the spin-dependent structure function of the 6-quark cluster reads

$$\bar{g}_1^6 = \int_0^1 g_1^6(z) dz = 0.189, \quad (31)$$

including only contributions of non-strange quarks. When the strange quark is also included, \bar{g}_1^6 becomes 0.162, which is compatible with that obtained by s -wave MIT bag wave functions [14].

Similar to the spin-independent case, the nuclear effect is described by the ratio

$$R_g^{D/N}(x) = g_1^D(x)/\tilde{g}_1^N(x) \quad (32)$$

and

$$\tilde{g}_1^N(x) = \frac{1}{2}[g_1^p(x) + \tilde{g}_1^n(x)]. \quad (33)$$

In our numerical calculation, g_1^D is taken from a fit to the E155 data [35], and g_1^p from a fit to the E143 data [36]. The ratio $R_g^{D/N}$, as shown in Fig. 4, is very different from the ratio $R_F^{D/N}$ (see Fig. 1), and it is also very different from that obtained in [13], where only Fermi motion corrections were considered, and whose result is independent of x over the wide range of $x = 10^{-3}$ –0.7, with a value of 0.9.

4.2 The effect on the Bjorken sum

Now, we turn to investigate the nuclear effect on the Bjorken sum [37]. This sum is defined as

$$S_{BS} = \int S_{BF}(x) dx, \quad (34)$$

with the Bjorken integrand function

$$S_{BF}(x) = g_1^p(x) - g_1^n(x). \quad (35)$$

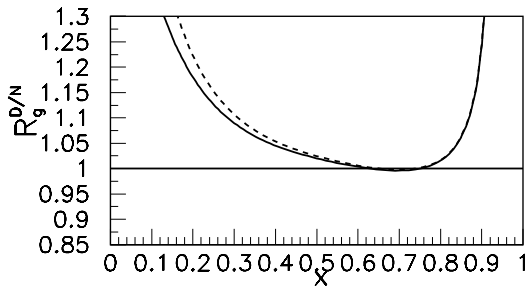


Fig. 4. The ratio $R_g^{D/N}(x)$. Dashed and solid curves correspond to including only contributions of non-strange quarks, and including also the contribution of the strange quark in the 6-quark cluster, respectively

There is also a Bjorken sum \tilde{S}_{BS} , and a Bjorken integrand function $\tilde{S}_{BF}(x)$, corresponding to the extracted \tilde{g}_1^n which includes nuclear effects.

The Bjorken sum rule with perturbative QCD correction to first order of α_s reads

$$S_{BS}^{\text{th}} = \frac{1}{6}g_A \left[1 - \frac{\alpha_s(Q^2)}{\pi} \right]. \quad (36)$$

With the well measured neutron beta decay coupling constant $g_A = 1.2601 \pm 0.0025$ [38] and very recently determined QCD coupling α_s [39] at $Q^2 = 4 \text{ GeV}^2$, one finds

$$S_{BS}^{\text{th}} \simeq 0.189. \quad (37)$$

In order to show the nuclear effect on the Bjorken integrand, we introduce the ratio

$$R_{BF}(x) = \frac{\tilde{S}_{BF}(x)}{S_{BF}(x)}, \quad (38)$$

whose value is larger than unity over the whole x region (see Fig. 5), therefore indicating an enhancement of the value of the Bjorken sum. Actually, the value of the sum changes from $S_{BS} = 0.167$ to $\tilde{S}_{BS} = 0.187$ when only the contribution of non-strange quarks in the 6-quark cluster is considered. When the strange quark in the 6-quark cluster is further included with $C_s = 3.8$, the Bjorken sum becomes 0.184, i.e., the nuclear effect results in an increase in the value of the Bjorken sum by about $\sim 10\%$. This value of the Bjorken sum is very close to the value in (37), the strict QCD prediction of the Bjorken sum rule. Therefore, the nuclear effect due to the presence of the 6-quark cluster favors the case in which the Bjorken sum rule holds. A very recent analysis by Cvetič and Kögerler [40] indicates that the above additional nuclear effect on the Bjorken sum has a significant effect on the determination of QCD coupling α_s .

4.3 The helium spin-dependent structure function g_1^{He}

The ${}^3\text{He}$ nucleus is a suitable system in which to check the above formalism for calculating the nuclear effect. Recently, some measurements on g_1^n have been made by using deep-inelastic scattering of polarized electrons on polarized ${}^3\text{He}$ [41–43]. In the simplest picture of ${}^3\text{He}$, all

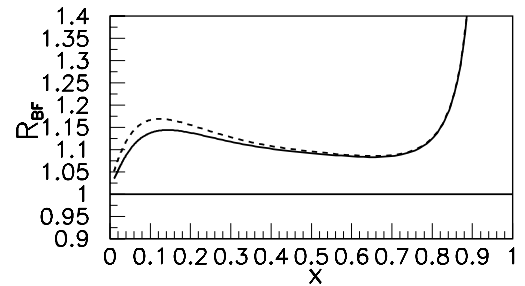


Fig. 5. The ratio $R_{BF}(x)$. Dashed and solid curves correspond to including only contributions of non-strange quarks, and including also the contribution of the strange quark in the 6-quark cluster, respectively

nucleons are in an S -wave, which consequently has a completely anti-symmetric spin-isospin wave function. The protons in ${}^3\text{He}$ are restricted by the Pauli principle to be in a spin-singlet state. It is usually believed that a polarized ${}^3\text{He}$ nucleus automatically provides a highly polarized neutron. We can use ${}^3\text{He}$ to have a self-consistent check for the extracted neutron spin-dependent structure function. ${}^3\text{He}$ is an isospin-1/2 nucleus in which the isovector clusters contribution to the ${}^3\text{He}$ spin-dependent structure function can be neglected and the isosinglet 6-quark clusters mainly come from the deuteron component of the ${}^3\text{He}$ wave function [14]. We assume that transporting the nuclear environment from deuterium to helium does not cause a distinct change in the quark spin structure of the 6-quark clusters. With the probabilities of 6-quark clusters in ${}^3\text{He}$ calculated by Benesh and Vary with the Bonn deuteron wave functions [14], we employ the extracted neutron spin-dependent structure function to predict the spin-dependent structure function of ${}^3\text{He}$. In Fig. 6a,b, the spin-dependent structure functions of the neutron and helium are shown, respectively, without the 6-quark clusters (dashed curve) and with the nuclear effect due to the presence of the 6-quark clusters (solid curve). We find that the calculated spin-dependent structure function of ${}^3\text{He}$ almost does not change, and therefore still provides a good fit to the experimental data (see Fig. 6b), although the neutron spin-dependent structure function gets a significant modification (see Fig. 6a). The contribution to the spin-dependent structure function of ${}^3\text{He}$ from the correction of the neutron spin-dependent structure function is almost canceled by that from 6-quark clusters. This means that we can also extract the same neutron spin-dependent structure function from the experimental data of g_1^{He} with the existence of 6-quark clusters in helium as that from g_1^D . This provides a good self-consistent check of our present framework.

5 Discussion and summary

For simplicity, only 6-quark clusters have been included in our approach. Inclusion of 9-quark clusters causes the maximum at $x \simeq 0.1$ to shift a little bit in Fig. 1. The calculations by Sato [44] show that the probability for

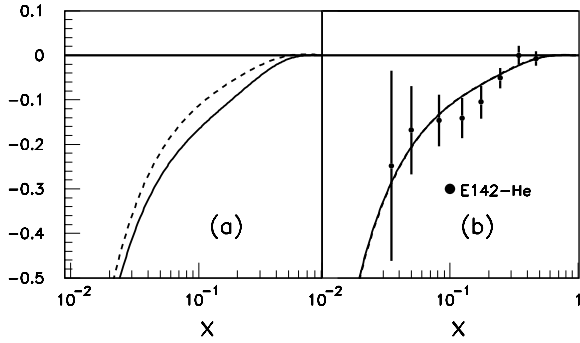


Fig. 6. **a** $g_1^n(x)$ and $\bar{g}_1^n(x)$; **b** $g_1^{\text{He}}(x)$ (dashed curve) and $\bar{g}_1^{\text{He}}(x)$ (solid curve). The dashed and solid curves correspond to not considering the 6-quark clusters and including the nuclear effect due to 6-quark clusters, respectively. Note that the dashed and solid curves in **b** almost overlap. The experimental data are taken from the E142 [43]

forming 9-quark clusters increases with the nuclear mass number A . In our present discussion of light nuclei, they can be neglected.

In our numerical calculation, $Q^2 = 4 \text{ GeV}^2$ was chosen in order to compare the results of the Gottfried sum with the experimental data of NMC [2]. This is also consistent with the kinematic range of the experiment in which the ratio $R_F^{\text{D/N}}(x)$ was extracted [4]. In principle, the present simple analytic representations of the quark distributions in 6-quark clusters only reflect the intrinsic bound-state structure of the 6-quark clusters and they are valid at low Q^2 where the QCD evolution can be neglected. At high Q^2 , the radiation from the struck quark line increases the effective power-law fall-off $(1-x)^p$ of the structure functions relative to the underlying quark distributions: $\Delta p = (4C_F/\beta_1) \log[\log(Q^2/\Lambda^2)/\log(Q_0^2/\Lambda^2)]$ [16], where $C_F = 4/3$ and $\beta_1 = 11 - (2/3)n_f$. With this estimate, the effect due to the scale change from $Q_0^2 = 1 \text{ GeV}^2$ to $Q^2 = 4 \text{ GeV}^2$ on our analysis is small. The quark distributions of the 6-quark cluster can be used as the input distribution for the perturbative QCD evolution from Q_0^2 to a higher resolution scale.

A model of the nuclear EMC effect should be grounded in the phenomenology of low energy nuclear physics. In principle, our analysis can be extended in order to consider the effect of 6-quark clusters on other observables such as form factors and magnetic moments. Further studies along this direction are in progress.

To sum up, we investigated the nuclear effects in light nuclei due the presence of 6-quark clusters. The quark distributions of the 6-quark clusters were modeled in the pQCD based framework. With the presence of the 6-quark clusters in the deuteron, our predictions of the nuclear effects including shadowing, anti-shadowing and Fermi motion, which are described by the ratio of the deuteron structure function to the free nucleon structure function, are consistent with the experimental data. The nuclear effects cause a decrease in the value of the Gottfried sum by about 7%. Then we extended the formalism for calculating the nuclear effects to the extraction of the spin-

dependent neutron structure function. We find that the nuclear effect on the extraction of the spin-dependent neutron structure function is more significant than that on the spin-independent neutron structure function. This effect results in an increase in the Bjorken sum by about 10%, which favors the strict QCD prediction of the Bjorken sum rule. A good self-consistent check of the formalism for calculating the nuclear effects was provided by evaluating the spin-dependent structure function of the ^3He nucleus.

Acknowledgements. This work is partially supported by Fondecyt (Chile) grant 3990048, 8000017 and by a Cátedra Presidencial (Chile), and by National Natural Science Foundation of China under Grant Numbers 19875024.

References

1. S. Kumano, Phys. Rep. **303**, 183 (1998), and references therein; hep-ph/9803359
2. New Muon Collaboration, M. Arneodo et al., Phys. Rev. D **50**, R1 (1994)
3. P. Amaudruz et al., Phys. Rev. Lett. **66**, 2712 (1991)
4. J. Gomez et al., Phys. Rev. D **49**, 4348 (1994)
5. European Muon Collaboration(EMC), J.J. Aubert et al., Phys. Lett. B **123**, 275 (1983)
6. Fermilab E665 Collaboration, M.R. Adams et al., Phys. Rev. Lett. **75**, 1466 (1995)
7. L.N. Epele, H. Fanchiotti, C.A. García Canal, R. Sassot, Phys. Lett. B **275**, 155 (1992)
8. I. Schmidt, R. Blankenbecler, Phys. Rev. D **16**, 1318 (1977)
9. V.V. Burov, A.V. Molochkov, Nucl. Phys. A **637**, 31 (1998)
10. E. Pace, G. Salmè, S. Scopetta, nucl-th/0009028
11. M.A. Braun, M.V. Tokarev, Phys. Lett. B **320**, 381 (1994)
12. A.V. Sidorov, M.V. Tokarev, Phys. Lett. B **358**, 353 (1995)
13. M.V. Tokarev, Phys. Lett. B **318**, 559 (1993)
14. C.J. Benesh, J.P. Vary, Phys. Rev. C **44**, 2175 (1991)
15. K.E. Lassila, U.P. Sukhatme, Phys. Lett. B **209**, 343 (1988)
16. S.J. Brodsky, M. Burkardt, I. Schmidt, Nucl. Phys. B **441**, 197 (1995)
17. M. Boglione, E. Leader, preprint VUTH-99-24 (1999), Phys. Rev. D **61**, 114001 (2000)
18. B.-Q. Ma, I. Schmidt, J.-J. Yang, hep-ph/9907556, USM-TH-81, Nucl. Phys. B **574**, 331 (2000)
19. B.-Q. Ma, I. Schmidt, J.-J. Yang, Phys. Lett. B **477**, 107 (2000)
20. B.-Q. Ma, I. Schmidt, J.-J. Yang, Phys. Rev. D **61**, 034017 (2000)
21. B.-Q. Ma, I. Schmidt, J. Soffer, J.-J. Yang, Eur. Phys. J. C **16**, 657 (2000)
22. R. Blankenbecler, S.J. Brodsky, Phys. Rev. D **10**, 2973 (1974); J.F. Gunion, Phys. Rev. D **10**, 242 (1974); S.J. Brodsky, G.P. Lepage, in Proceedings 1979 Summer Inst. on Particle Physics, SLAC (1979)
23. U. Stiegler, Phys. Rep. **277**, 1 (1996)
24. A.D. Martin, W.J. Stirling, R.G. Roberts, Phys. Lett. B **306**, 145 (1993); Phys. Rev. D **50**, 6734 (1994)
25. NMC Collaboration, M. Arneodo et al., Phys. Lett. B **364**, 107 (1995)

26. L.L. Frankfurt, M.I. Strikman, Phys. Rep. **160**, 235 (1988)
27. F.E. Close, J. Qiu, R.G. Roberts, Phys. Rev. D **40**, 2820 (1989)
28. S. Kumano, Phys. Rev. C **48**, 2016 (1993)
29. J.J. Yang, G.L. Li, Z. Phys. C **76**, 287 (1997)
30. K. Gottfried, Phys. Rev. Lett. **18**, 1174 (1967)
31. W. Melnitchouk, A.W. Thomas, Phys. Rev. D **47**, 3783 (1993)
32. W. Melnitchouk, A.W. Thomas, Phys. Lett. B **377**, 11 (1996)
33. Bo-Qiang Ma, Phys. Lett. B **375**, 320 (1996)
34. G.R. Farrar, D.R. Jackson, Phys. Rev. Lett. **35**, 1416 (1975)
35. SLAC E155, P.L. Anthony et al., Phys. Lett. B **463**, 339 (1999)
36. SLAC E143 Collaboration, K. Abe et al., Phys. Rev. Lett. **74**, 346 (1995)
37. J.D. Bjorken, Phys. Rev. **148**, 1467 (1966); Phys. Rev. D **1**, 1376 (1970)
38. Particle Data Group, R.M. Barnett et al., Phys. Rev. D **54**, 1 (1996)
39. S. Bethke, hep-ex/0004021
40. G. Cvetič, R. Kögerler, Phys. Rev. D **63**, 056013 (2001)
41. SLAC E154 Collaboration, K. Abe et al., Phys. Rev. Lett. **79**, 26 (1997)
42. The HERMES Collaboration, K. Ackerstaff et al., Phys. Lett. B **404**, 383 (1997)
43. SLAC E142, P.L. Anthony et al., Phys. Rev. D **54**, 6620 (1996)
44. M. Sato, S.A. Coon, H.J. Pirner, J.P. Vary, Phys. Rev. C **33**, 1062 (1986)